Biosensors and Bioelectronics 151 (2020) 111985

Contents lists available at ScienceDirect

Biosensors and Bioelectronics

journal homepage: http://www.elsevier.com/locate/bios

Sensitive detection of low-concentration sulfide based on the synergistic effect of rGO, np-Au, and recombinant microbial cell

Congcong Bian, Huimin Wang, Xueli Zhang, Sa Xiao, Zhuang Liu, Xia Wang *

State Key Laboratory of Microbial Technology, Shandong University, Qingdao, 266237, PR China

ARTICLE INFO

Keywords:
Sulfide
Microbial biosensor
Synergistic effect
Composite

ABSTRACT

With the aggravation of sulfide pollution, more and more attention has been paid to the detection of sulfide in the environment. However, the detection of low-concentration sulfide is still a technical bottleneck to be solved urgently. In this study, a synergistic effect strategy that combines the co-catalysis of nanoporous gold (np-Au) and recombinant microbial cell with the excellent electrical conductivity of reduced graphene oxide (rGO) was proposed for the sensitive detection of low-concentration sulfide. A rGO/np-Au composite was fabricated and then used as an immobilization support for the bio-recognition element of recombinant *Escherichia coli* (*E. coli*) over-expressed sulfide: quinone oxidoreductase (SQR). A microbial biosensor (*E. coli*^{SQR}/rGO/np-Au/GCE) was successfully constructed for the sensitive detection of low-concentration sulfide. Due to the synergistic effect of rGO, np-Au, and *E. coli*^{SQR} cells, the sensitivity of the proposed microbial biosensor towards sulfide reached 400.42 μA mM^{-1} cm^{-2} with a wide linear response ranging from 100 nM to 7 mM, as well as a low detection limit of 98.5 nM using amperometric i-t curve method. Furthermore, the microbial biosensor was successfully applied to the detection of sulfide in wastewater with strong anti-interference ability, high reproducibility, and strong stability. These results confirmed that the proposed microbial biosensor was ideal for the detection of low-concentration sulfide in a reliable, specific, and sensitive way.

1. Introduction

In recent years, sulfide pollution has caused serious environmental and health issues (Liu et al., 2012) because of its strong odor and toxicity. Thus, sulfide was used as one of the important indicators to evaluate the quality of the environment. Among sulfides, hydrogen sulfide (H_2S) is a major kind of toxic sulfides that impose threat to human health. Low concentration, even trace amount of hydrogen sulfide, can cause headache, dizziness, and other physical discomforts (Milby and Baselt, 1999; Ma et al., 2006; Liu et al., 2017). Therefore, the sensitive detection of sulfide in environmental samples has attracted wide attention. For sulfide analysis, some methods, such as fluorescent probe (Liu et al., 2012; Peng et al., 2014; Yu et al., 2014), gas chromatography-mass spectrometry (Vycudilik, 1985), potentiometric (García-Calzada et al., 1999), ion exchange (Van Staden and Kluever, 1998), and biosensors (Xu et al., 2016; Liu et al., 2017), have been successfully developed. Among these methods, biosensor, as a simple, specific, sensitive, rapid, and portable approach, is being evaluated where living systems are used for environmental sample bioassays (Liu et al., 2013, 2017; Lu et al., 2014, 2015; Poor et al., 2014; Zhang et al., 2015). However, it is very difficult to detect sulfide at low concentration or trace grade in actual environmental samples by biosensor at present.

Among biosensors, microbial biosensor has attracted the attention of many researchers because whole cells are simple and inexpensive systems to construct the biosensor and enzymes are usually more stable in their natural environment in the cell (Canbay et al., 2015; Hui et al., 2017). Microbial biosensor is generally an immobilized cell that is combined with a transducer or an immobilizing support to monitor a specific change in the microenvironment (Kumar and D'Souza, 2011). However, the poor conductivity of microbial cells leads to the low sensitivity of microbial biosensor. Therefore, the transducer or immobilization materials play a key role in improving the sensitivity of microbial biosensor. With the development of nanomaterials, the low sensitivity of microbial biosensors caused by the poor conductivity of microbial cells may be solved by using nanomaterials as transducers or immobilization materials (Xu et al., 2016; Zhang et al., 2017; Hui et al., 2017). Among nanomaterials, reduced graphene oxide (rGO) is an ideal electrode modified material that not only retains strong conductivity

* Corresponding author.
E-mail address: ghwx@sdu.edu.cn (X. Wang).

https://doi.org/10.1016/j.bios.2019.111985
Received 24 October 2019; Received in revised form 9 December 2019; Accepted 22 December 2019
Available online 26 December 2019

and large specific surface area of graphene, but also has good biocompatibility and stability after oxidation-reduction process (Chang et al., 2014; Cui et al., 2015). Additionally, nano-porous metal materials, such as nano-porous gold (np-Au) with three-dimensional bi-continuous nano-porous sponge structure, could provide a good microenvironment to stabilize the biocomponents in what is often an unnatural environment while retaining their functions and activities (Wang et al., 2011; Feng et al., 2017). Further, as an electrocatalyst, np-Au could catalyze the reaction of some substances, such as nitrite (Ge et al., 2011), glucose (Wu et al., 2016), carbendazim (Gao et al., 2019), and sulfide (Liu et al., 2017) due to its good electrocatalysis properties. Combining the unique physicochemical properties of rGO and np-Au, the composite of rGO/np-Au may be an ideal transducer or supporting material for microbial cells immobilization, which could achieve the sensitive detection of low-concentration sulfide.

Because of high specificity and catalytic activity, enzymes have become the main bio-recognition elements for sulfide detection. In the family of sulfide catalytic oxidases, sulfide:quinone oxidoreductase (SQR), isolated from hyperthermoacidophilic archaeon *Acidianus ambivalens*, exhibits high catalytic activity towards sulfide (Xin et al., 2016). Furthermore, SQR is a membrane protein that allows it to be displayed on the surface of *Escherichia coli* (*E. coli*) cells by recombination technology (Brito et al., 2009), which is beneficial to the construction of microbial cell biosensor when whole cells are used as the recognition element. Owing to its high specific activity and membrane protein characteristics, SQR makes it possible to construct a sensentive microbial biosensor for low-concentration sulfide detection.

In this study, a synergistic effect strategy was proposed for the sensitive detection of low-concentration sulfide based on the co-catalysis of np-Au and recombinant *E. coli* cells over-expressed SQR and the excellent electrical conductivity of rGO as illustrated in Scheme 1. rGO/np-Au composite with both catalytic activity and good electron transfer capability was prepared and then used as electrode modified material and supporting material for the recombinant *E. coli*^{SQR} cells immobilization. The sensitivity of the proposed microbial biosensor was significantly improved based on the synergistic effect strategy of rGO, np-Au, and *E. coli*^{SQR} cells in low-concentration sulfide detection.

2. Experimental

2.1. Regents and materials

The purity nitrogen (purity > 99.9%) was acquired from Yantai Deyi-Qiti Co., Ltd. (Yantai, China). rGO was purchased from Chengdu Organic Chemicals Co., Ltd., Chinese Academy of Sciences (Chengdu, China). The powder of Al_2O_3 (diameter is 50 nm) was purchased from CH Instruments, USA. Ultrapure water (resistivity greater than 18 MΩ cm) was made by an ultra-pure water machine (Milli-Q) and used throughout the experiments.

Phosphate buffer solution (PBS, 50 mM, pH 7.5) was made up with moderate amounts of $Na_2HPO_4{\cdot}12H_2O$ and $NaH_2PO_4{\cdot}2H_2O$. Sodium sulfide was dissolved in PBS (50 mM, pH 7.5) to prepare 100 mM sodium sulfide solution.

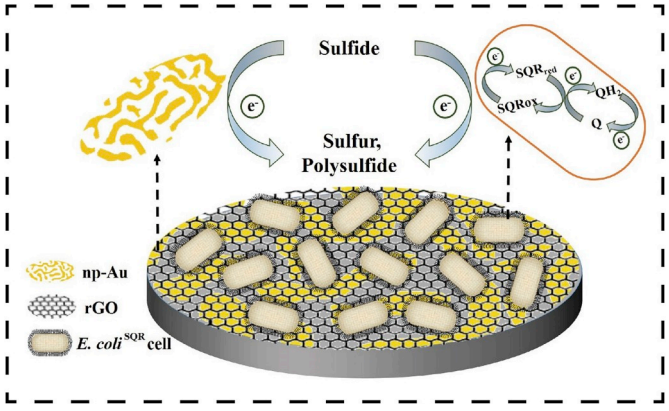

Scheme 1. The electrochemical reaction principle of the *E. coli*^{SQR}/rGO/np-Au/GCE bioelectrode.

2.2. The modification of GCE by np-Au and rGO

Glassy carbon electrode (GCE) was polished on a piece of chamois leather using Al_2O_3 powder with a diameter of 50 nm. The electrode was cleaned ultrasonically in absolute ethyl alcohol and ultrapure water for 30 s, respectively. np-Au was prepared by a chemical dealloying method as described previously (Wang et al., 2011). After that, the mirror-polished GCE was coated with np-Au thin film (~100 nm thick) to construct np-Au/GCE electrode in ultrapure water. The prepared np-Au/GCE electrode was stored in a dustproof cupboard.

For rGO/np-Au/GCE electrode construction, rGO suspension (0.1%, w/v) was made by adding an appropriate amount of rGO powder in anhydrous ethanol with an ultrasonic dispersion for 30 min. The np-Au/GCE electrode was loaded with 12 μL rGO suspension (0.1%, w/v) and dried at room temperature for 24 h. Nafion solution (2 μL, 0.5%, v/v) was dropped on the surface of the rGO/np-Au/GCE electrode to prevent rGO from falling off. The prepared rGO/np-Au/GCE electrode was stored at 4 °C in a refrigerator.

2.3. The immobilization of E. coli^{SQR} cells

The construction of recombinant *E. coli*^{SQR} cells was described in our previous study (Liu et al., 2017). The *E. coli*^{SQR} cells culture (1 mL) was centrifuged at 8000 rpm for 5 min, and then the precipitation was resuspended using PBS (50 mM, pH 7.5). An appropriate amount of the resuspended suspension was added on the surface of the rGO/np-Au/GCE electrode to construct an *E. coli*^{SQR}/rGO/np-Au/GCE bioelectrode. After 24 h immobilization, the unfixed microbial cells were removed by ultrapure water. Then, the prepared *E. coli*^{SQR}/rGO/np-Au/GCE bioelectrode was covered with 2 μL Nafion solution (0.5%, v/v).

2.4. Experimental measurements

Electrochemical experiments were performed in a conventional three-electrode system at 25 °C by an electrochemical workstation (CHI 760E, Shanghai Chenhua Apparatus Corporation, China). Pt electrode sheet (1 cm × 1 cm) was used as a counter electrode and saturated calomel electrode (SCE) was used as a reference electrode. The GCE electrode, np-Au/GCE electrode, rGO/np-Au/GCE electrode, and *E. coli*^{SQR}/rGO/np-Au/GCE bioelectrode was used as working electrode, respectively. Electrolyte solution (15 mL PBS, 50 mM, pH 7.5) was deoxygenated by N_2 for 10 min before each electrochemical experiment. N_2 was filled throughout each electrochemical measurement system, and all potentials were referred to SCE.

3. Results and discussion

3.1. Catalytic activity of recombinant E. coli^{SQR} cells

The catalytic oxidation activity of the recombinant *E. coli*^{SQR} cells towards sulfide was detected by a methylene blue spectrophotometric method. A certain amount of recombinant *E. coli*^{SQR} cells liquid was mixed with an appropriate amount of sodium sulfide to make a reaction system, and wild *E. coli* cells liquid served as a control at the same condition. The catalytic reaction was carried out at 25 °C for 60 s. As shown in Fig. 1A–a, the absorbance of the wild *E. coli* cells reaction system did not change. Accordingly, the color of the wild *E. coli* cells reaction system did not show obvious change during 60 s reaction

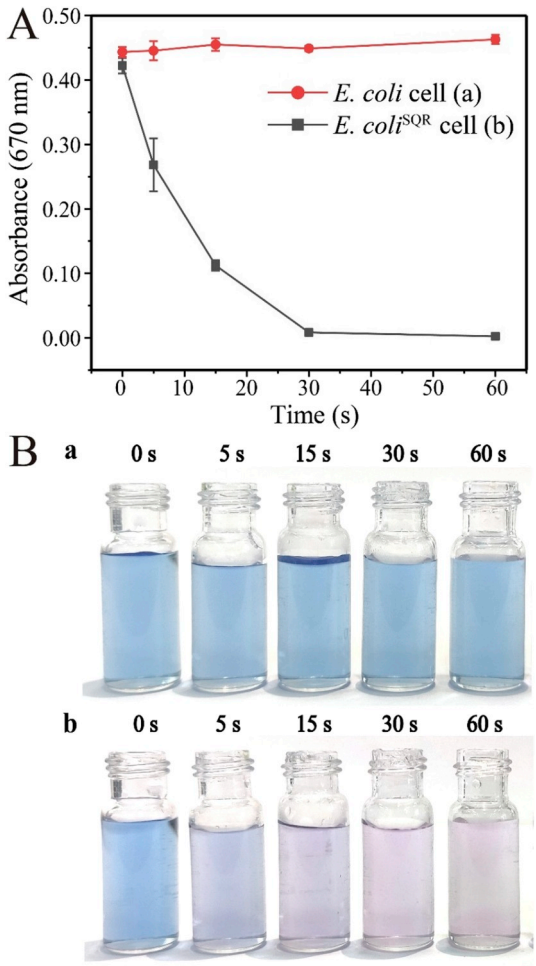

Fig. 1. (A) The absorbances of wild *E. coli* cells reaction system (a) and *E. coli*^{SQR} cells reaction system (b) as a function of time. (B) The colors of wild *E. coli* cells reaction system (a) and *E. coli*^{SQR} cells reaction system (b) as a function of time. (For interpretation of the references to color in this figure legend, the reader is referred to the Web version of this article.)

process (Fig. 1B–a). These results indicated that the wild *E. coli* cells have no catalytic activity towards sulfide. In contrast, the absorbance of the recombinant *E. coli*^{SQR} cells reaction system decreased rapidly from 0.43 to 0 AU at 670 nm (A_{670}) at 30 s (Fig. 1A–b). Meanwhile, the color of the recombinant *E. coli*^{SQR} cells reaction system changed from blue to pink as shown in Fig. 1B–b. These results confirmed that the recombination *E. coli*^{SQR} cells presented high catalytic activity towards sulfide, which indicated that they could be used as bio-recognition elements to construct a microbial biosensor for sulfide detection in subsequent experiments.

3.2. Characterization of *E. coli*^{SQR}/rGO/np-Au/GCE bioelectrode

Based on above results, a microbial biosensor (*E. coli*^{SQR}/rGO/np-Au/GCE) was successfully constructed for the sensitive detection of low-concentration sulfide according to Scheme 1. First, the morphologies of the np-Au/GCE electrode, rGO/np-Au/GCE electrode, and *E. coli*^{SQR}/rGO/np-Au/GCE bioelectrode were characterized by a scanning electron microscopy (SEM, JSM6700F), respectively. The inset of Fig. 2A shows that np-Au has a three-dimensional bi-continuous nano-porous sponge structure with average ligaments and pore dimension around 35 nm, indicating that it possesses relatively large specific surface area and more reactive sites (Gao et al., 2019). The rGO arranged randomly on the surface of np-Au has a single lamellar structure with wrinkles

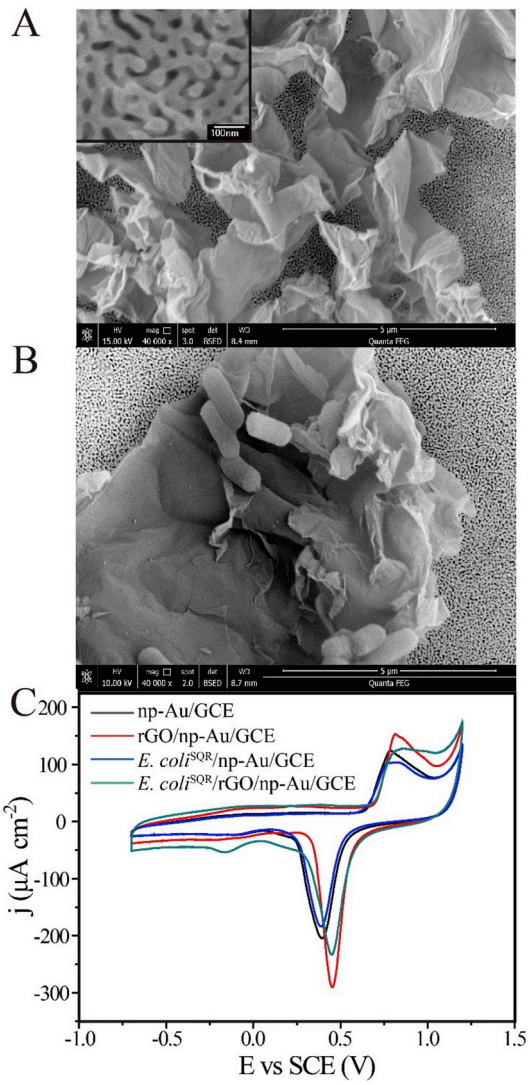

Fig. 2. The SEM images of rGO/np-Au/GCE electrode before (A) (Inset is np-Au SEM image) and after (B) *E. coli*^{SQR} cells loading. (C) The CVs of np-Au/GCE electrode, rGO/np-Au/GCE electrode, *E. coli*^{SQR}/np-Au/GCE bioelectrode, and *E. coli*^{SQR}/rGO/np-Au/GCE bioelectrode in deoxygenated PBS (50 mM, pH 7.5).

(Fig. 2A), which provides more binding sites for *E. coli*^{SQR} cells immobilization. It is easy to observe that *E. coli*^{SQR} cells are adsorbed on the surface of rGO/np-Au composite as shown in Fig. 2B, and the length and diameter of *E. coli*^{SQR} cell are about 4 μm and 2 μm, respectively. These results confirmed that the *E. coli*^{SQR}/rGO/np-Au/GCE bioelectrode was constructed successfully. After the morphology characterization, the electrochemical behaviors of the np-Au/GCE electrode, rGO/np-Au/GCE electrode, *E. coli*^{SQR}/np-Au/GCE bioelectrode, and *E. coli*^{SQR}/rGO/np-Au/GCE bioelectrode were compared using cyclic voltammogram (CV). The experiments were explored in 15 mL deoxygenated PBS (50 mM, pH 7.5) by CV at a scan rate of 50 mV s^{-1}. As illustrated in Fig. 2C, the redox peak current densities of the rGO/np-Au/GCE electrode were higher than those of the np-Au/GCE electrode at +0.9 V and +0.4 V, respectively (Fig. 2C), indicating that the rGO on np-Au surface accelerated electron transfer due to its rich π-conjugation structure (Becerril et al., 2008), which in turn increased the electrochemical response of np-Au. In contrast, the redox peak current densities of np-Au all decreased for the *E. coli*^{SQR}/np-Au/GCE and *E. coli*^{SQR}/rGO/np-Au/GCE bioelectrodes, which was caused by the poor electrical conductivity of *E. coli*^{SQR} cells. Moreover, the redox peak current densities of the *E. coli*^{SQR}/rGO/np-Au/GCE bioelectrode were

significantly higher than those of the *E. coli*^{SQR}/np-Au/GCE bioelectrode and equivalent to those of the np-Au/GCE electrode, which supported that rGO significantly increased the electron transport capability of the *E. coli*^{SQR}/rGO/np-Au/GCE bioelectrode (Manavalan et al., 2019). It could be concluded from these results that the sensing performance of the *E. coli*^{SQR}/rGO/np-Au/GCE bioelectrode could be significantly improved when the rGO/np-Au composite served as a supporting material for the *E. coli*^{SQR} cells immobilization.

3.3. The sensing performance of *E. coli*^{SQR}/rGO/np-Au/GCE bioelectrode

Based on above assumption, the electrochemical responses of the *E. coli*^{SQR}/rGO/np-Au/GCE bioelectrode, rGO/np-Au/GCE electrode, np-Au/GCE electrode, and bare GCE electrode towards sulfide were evaluated in deoxygenated PBS (50 mM, pH 7.5) containing 100 μM sodium sulfide using differential pulse voltammetry (DPV). As shown in Fig. 3A, the oxidation peak was observed around −0.24 V for sodium sulfide. For the same concentration of sodium sulfide, the *E. coli*^{SQR}/rGO/np-Au/GCE bioelectrode exhibited the highest oxidation peak current density, followed by the rGO/np-Au/GCE electrode, and the np-Au/GCE electrode has the lowest oxidation peak current density (Fig. 3A). These results verified our previous assumption that the sensitivity of the *E. coli*^{SQR}/rGO/np-Au/GCE bioelectrode could be significantly improved by combining the co-catalysis of np-Au and recombinant *E. coli*^{SQR} cells with the excellent electrical conductivity of rGO. Firstly the surface of rGO/np-Au composite with folding structure can provide sufficient binding sites for *E. coli*^{SQR} cells immobilization.

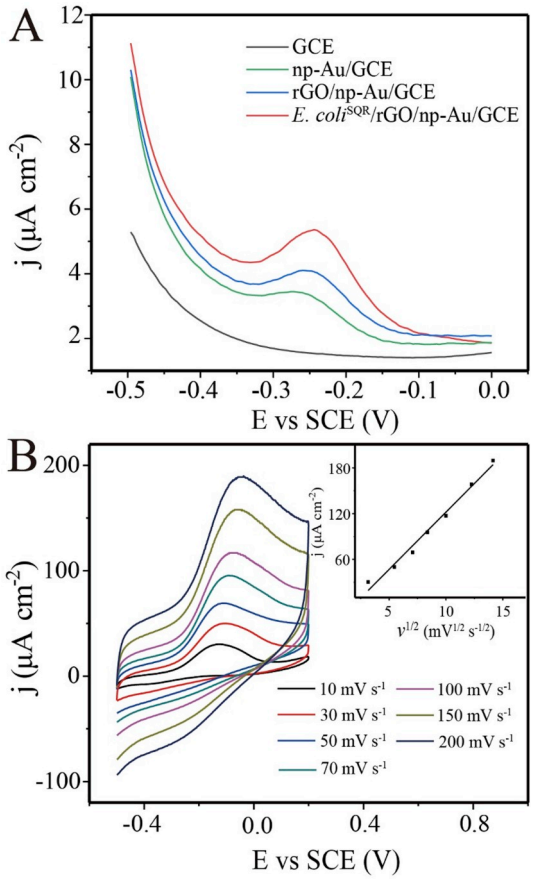

Fig. 3. (A) The DPVs of GCE electrode, np-Au/GCE electrode, rGO/np-Au/GCE electrode, and *E. coli*^{SQR}/rGO/np-Au/GCE bioelectrode in deoxygenated PBS (50 mM, pH 7.5) with 100 μM sodium sulfide. (B) The CVs of *E. coli*^{SQR}/rGO/np-Au/GCE bioelectrode at different scan rates in deoxygenated PBS (50 mM, pH 7.5) with 200 μM sodium sulfide, the inset profile shows the peak current density as a function of the square root of scan rate.

Second, due to the excellent electrical conductivity (10^6 S cm^{-1}) and high charge mobility (200 000 cm^2 V^{-1} s^{-1}) of rGO, the electrons generated in catalytic reaction can be efficiently transferred to the electrode (Allen et al., 2010; Dai, 2013). Finally, the co-catalytic capability of np-Au and recombination *E. coli*^{SQR} cells towards sulfide is significantly higher than that of np-Au or recombination *E. coli*^{SQR} cells alone.

3.4. The reaction mechanism of *E. coli*^{SQR}/rGO/np-Au/GCE bioelectrode

Sulfide (main forms in deoxygenated PBS are HS^- and S^{2-}) might be oxidized to polysulfide and elemental sulfur directly by a biocatalyst such as SQR or an electrocatalyst such as np-Au according to previous reports (Alfonso, 2008; Xin et al., 2016; Liu et al., 2017).

For the microbial biosensor constructed in this study, a synergistic effect strategy was proposed for the sensitive detection of low-concentration sulfide by combining the co-catalysis of np-Au and SQR over-expressed on the membrane of *E. coli* cells with the excellent electrical conductivity of rGO. As an ideal electrode modified material, rGO played a key role in improving the sensitivity of the microbial biosensor due to its excellent electrical conductivity. The detection principle of the microbial biosensor was that sulfide could be oxidized to polysulfide and elemental sulfur by the co-catalysis of np-Au and SQR over-expressed on the membrane of *E. coli* cells as described previously (Xin et al., 2016; Liu et al., 2017).

The working principle of np-Au could be described as follows:

$$HS^-(S^{2-}, H_2S) \overset{np-Au}{\rightarrow} S^0 + 2e^- \quad (1)$$

The working principle of *E. coli*^{SQR} cells towards sulfide could be demonstrated as follows:

$$HS^-(S^{2-},\ H_2S) + SQR_{ox}(FAD) + 2H^+ \rightarrow S^0(polysulfide) + SQR_{red}(FADH_2) \quad (2)$$

$$SQR_{red}(FADH_2) + Q \rightarrow SQR_{ox}(FAD) + QH_2 \quad (3)$$

$$QH_2 \overset{bioelectrode}{\rightarrow} Q + 2e^- + 2H^+ \quad (4)$$

In the electrochemical catalysis of sulfide, SQR could catalyze the oxidation reduction of sulfide and ubiquinone (Q), respectively (Cherney et al., 2010; Zhang et al., 2016). In this process, a $FADH_2$ was produced by a FAD cofactor capturing two electrons from a sulfide ion. Meanwhile, an oxidized state SQR_{ox} was changed into a reduced state SQR_{red}. Next, dihydroubiquinone (QH_2) was produced by Q obtained two electrons from the $FADH_2$. Accordingly, the $FADH_2$ was oxidized to FAD. Subsequently, the SQR_{red} was oxidized to the SQR_{ox}. Obviously, the Q/QH_2 couple acted as an ideal electron mediator in this electrochemical reaction (Qiu et al., 2012; Wu et al., 2016). As described in Eq. (4), QH_2 would be reduced back to Q by the bioelectrode. During the electrochemical catalysis of sulfide, FAD and Q are provided by the host (namely *E. coli* cell) of SQR. The oxidation reaction process of sulfide on the surface of the *E. coli*^{SQR}/rGO/np-Au/GCE bioelectrode was illustrated detailly in Scheme 1.

In order to explore sulfide oxidation reaction kinetics on the surface of the *E. coli*^{SQR}/rGO/np-Au/GCE bioelectrode, the bioelectrode was investigated using CV under the scan rates from 10 to 200 mV s^{-1} in deoxygenated PBS (50 mM, pH 7.5) containing 200 μM sodium sulfide. It can be seen that the peak potential shifted slightly toward positive direction with increasing scan rate. A linear relationship between the square root of the scan rate ($v^{1/2}$) and the peak current density of the *E. coli*^{SQR}/rGO/np-Au/GCE bioelectrode was observed with a correlation coefficient of 0.993 (see the inset of Fig. 3B). These results confirmed that the electrochemical oxidation reaction of sulfide was an diffusion controlled process on the surface of the *E. coli*^{SQR}/rGO/np-Au/GCE bioelectrode (Jin et al., 2014).

3.5. Electrochemical detection of sulfide

All above results indicated that the sensitivity of the *E. coli*^{SQR}/rGO/np-Au/GCE bioelectrode was significantly improved based on the synergistic effect of rGO, np-Au, and *E. coli*^{SQR} cells. The electrochemical detection of sulfide by the *E. coli*^{SQR}/rGO/np-Au/GCE bioelectrode was evaluated detailly using amperometric i-t curve method. For the amperometric i-t curve analysis, −0.24 V was selected to be the applied potential for sulfide detection because a fast and well-defined response towards sulfide was observed at the potential of −0.24 V (Fig. 3A). As shown in Fig. 4A, the current response increased with the sulfide concentration increases in a widespread range from 100 nM to 7 mM. Moreover, the plot of the peak current density associated with sulfide concentration was comprised of two linear relationships with different slopes as illustrated in Fig. 4B and C. When the concentration increased from 100 nM to 20 μM, the linear regression equation was $j(\mu A\ cm^{-2}) = 0.40042 \times C_{sulfide}(\mu M) - 10.30522$ ($R^2 = 0.993$) with a high sensitivity of 400.42 μA mM^{-1} cm^{-2} (Fig. 4B). With the concentration ranging from 20 μM to 7 mM, the linear regression equation could be exhibited as $j(\mu A\ cm^{-2}) = 0.00546 \times C_{sulfide}(\mu M) - 0.88183$ ($R^2 = 0.984$) with a sensitivity of 5.46 μA mM^{-1} cm^{-2} (Fig. 4C). The detection limit of sulfide was calculated as low as 98.5 nM according to the equation: $C_L = 3 \times Sd/k$, where C_L is the detection limit, Sd (0.01315 μA cm^{-2}) is the standard deviation of the blank response, and k is the slope of the calibration plot (Yan et al., 2011). The reason for two linear relationships with different slopes may be demonstrated as follows. At low sulfide concentrations, the local concentration on the bioelectrode surface is exhausted rapidly as the substrate is converted into product by the co-catalysis of np-Au and SQR, resulting in a high sensitivity of the bioelectrode. At higher sulfide concentrations, the substrate supply for the electrochemical catalyst such as np-Au and SQR needs a longer period of time and the electrochemical reaction proceeds over a larger time window (Dong et al., 2015), which, together with the fouling of the bioelectrode surface caused by the products, results in a lower sensitivity of the bioelectrode. Thus, the microbial biosensor exhibited two linear relationships with different slopes, which is consistent with the previous report that there were two linear correlations at different concentration ranges in the detection of H_2O_2 (Dong et al., 2015).

Additionally, compared to other detection systems illustrated in supporting information (Table S1), the *E. coli*^{SQR}/rGO/np-Au/GCE bioelectrode exhibited better sensing performance in low concentration sulfide detection, which also confirmed that the sensitivity of the *E. coli*^{SQR}/rGO/np-Au/GCE bioelectrode was significantly improved.

3.6. Anti-interference, reproducibility, and stability of bioelectrode

The anti-interference capability is an important index for evaluating the performance of a biosensor. Therefore, sulfur-containing compound such as dimethyl sulfoxide (DMSO), L-methionine (L-Met), dibenzothiophene (DBT), and glutathione (GSH) and common pollutants in wastewater such as catechol (Cat) and biphenyl (BP) were used to assess the anti-interference capability of the *E. coli*^{SQR}/rGO/np-Au/GCE bioelectrode. In the anti-interference experiment, DMSO, L-Met, DBT, GSH, Cat, and BP were added into 15 mL deoxygenated PBS (50 mM, pH 7.5) containing 200 μM sodium sulfide, and the concentration ratio of each interferent to sodium sulfide was 2.5:1, respectively. As illustrated in Fig. 4D, after adding these interferents, the peak current densities changed 0.5%, 3.0%, 0.07%, 1.7%, 3.9%, 0.23% for DMSO, L-Met, DBT, GSH, Cat, and BP, respectively. The deviation rates were all less than 3.9% at the existence of these common interfering substances, which demonstrated that the *E. coli*^{SQR}/rGO/np-Au/GCE bioelectrode had excellent anti-interference property in low-concentration sulfide

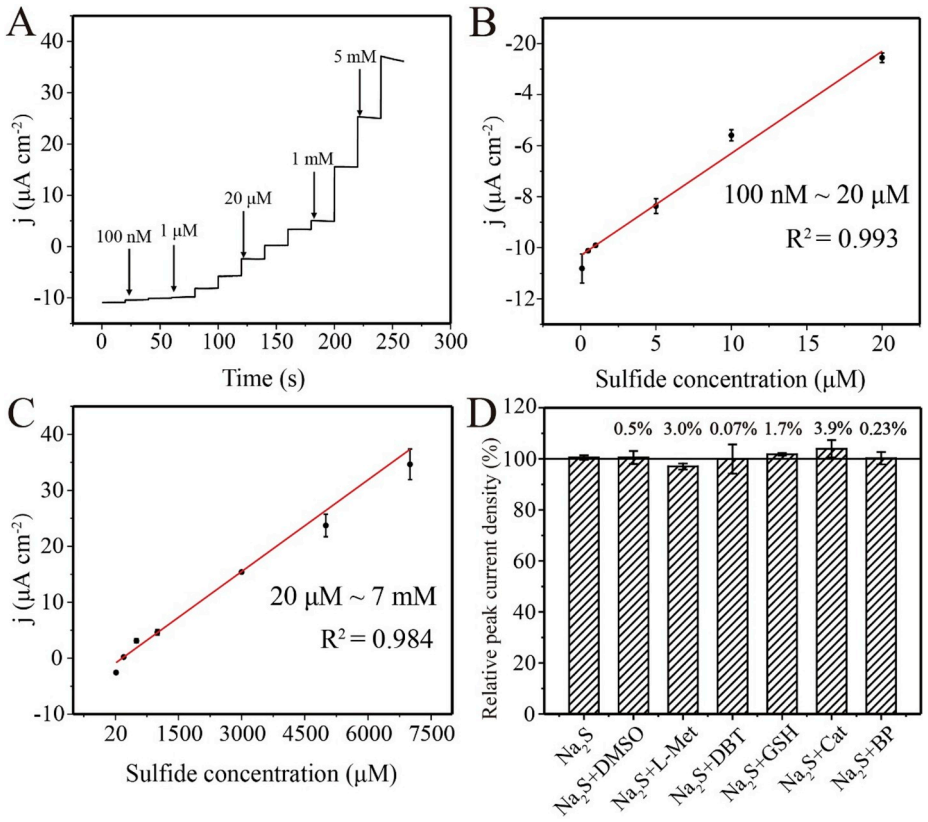

Fig. 4. (A) The amperometric i-t responses of the *E. coli*^{SQR}/rGO/np-Au/GCE bioelectrode towards sulfide at a regular interval time of 20 s. (B) and (C) are the calibration curves between peak current density and sulfide concentration; (B) is for the concentration ranged from 100 nM to 20 μM, and (C) is for the concentration ranged from 20 μM to 7 mM. (D) The effects of interferents on sulfide detection.

Table 1
The determination of sulfide in wastewater samples.

Sample	Added Na_2S	Proposed biosensor	Recovery (%)	Deviation rate (%)
1	0.3 μM	296.28 ± 5.89 nM	98.76	−1.24
2	0.5 μM	492.89 ± 3.41 nM	98.57	−1.43
3	35 μM	36.78 ± 0.55 μM	105.07	+5.07
4	55 μM	54.31 ± 0.24 μM	98.73	−1.27
5	200 μM	191.29 ± 8.34 μM	95.65	−4.35
6	500 μM	493.12 ± 0.84 μM	98.63	−1.37

detection.

The reproducibility was also explored in deoxygenated PBS (50 mM, pH 7.5) containing 200 μM sodium sulfide. By means of the 5 repetitive measurements, the *E. coli*^{SQR}/rGO/np-Au/GCE bioelectrode exhibited a favorable repeat performance with a relative standard deviation (RSD) of 4.7% (n = 5). This result confirmed that the bioelectrode was feasible in the sulfide detection of wastewater with high reproducibility.

The stabilization of the microbial biosensor is a fundamental element for sulfide detection. In order to study stabilization, the *E. coli*^{SQR}/rGO/np-Au/GCE bioelectrode was stored at 4 °C in a refrigerator, and the electrochemical response of the bioelectrode towards 200 μM sodium sulfide was detected weekly. The results showed that the *E. coli*^{SQR}/rGO/np-Au/GCE bioelectrode still remained 88.4% of its original electrochemical response after one-month storage, indicating a favorable stability for the *E. coli*^{SQR}/rGO/np-Au/GCE bioelectrode.

3.7. Detection of sulfide in wastewater

To explore its application performance in environmental wastewater, the *E. coli*^{SQR}/rGO/np-Au/GCE bioelectrode was used to detect sulfide in wastewater samples provided by Jining wastewater treatment plant (Jining, China). First, sulfide in wastewater sample was detected by the *E. coli*^{SQR}/rGO/np-Au/GCE bioelectrode. It was found that there was no electrochemical response observed, demonstrating that the wastewater sample provided by Jining wastewater treatment plant did not contain sulfide. Subsequently, the linear relationship between peak current density and sulfide concentration in diluted wastewater (the ratio of wastewater to PBS was 1:4) was explored by the *E. coli*^{SQR}/rGO/np-Au/GCE bioelectrode using amperometric i-t curve method. The results showed that two good linear relationships with different slopes were also observed in a wide linear response ranging from 500 nM to 3 mM with a high sensitivity of 405.21 μA mM^{-1} cm^{-2} as well as a low detection limit of 97.3 nM (Fig. S1, supporting information). Besides, the recovery experiments were carried out by adding different amounts of sodium sulfide (300 nM ~ 500 μM) in the wastewater sample. The comparison between the standard concentrations and the concentrations detected by the *E. coli*^{SQR}/rGO/np-Au/GCE bioelectrode was listed in Table 1. The recovery of sodium sulfide in wastewater samples ranged from 95.65% to 105.07%, while the deviation rates was less than 5.07%. Further, the sodium sulfide concentration as low as nano-mole can be successfully detected by the *E. coli*^{SQR}/rGO/np-Au/GCE bioelectrode, which met the requirements for the detection of low-concentration sulfide in the environment.

4. Conclusion

In summary, a highly sensitive microbial biosensor for low-concentration sulfide detection is successfully constructed based on the synergistic effect strategy of rGO, np-Au, and *E. coli*^{SQR} cells. It was observed that the proposed microbial biosensor could detect sulfide with a low detection limit of 98.5 nM. The sensitivity of the proposed microbial biosensor towards sulfide reached 400.42 μA mM^{-1} cm^{-2} in a wide linear response ranging from 100 nM to 7 mM. Due to the unique structural and functional features of the rGO/np-Au composite and the co-catalytic capability of np-Au and recombination *E. coli*^{SQR} cells towards sulfide, the sensitivity of the proposed microbial biosensor was significantly improved with high anti-interference ability, good reproducibility, and strong stability. These distinctive features make the microbial biosensor a reliable method in low-concentration sulfide detection in the environment.

Declaration of competing interest

The authors declare that they have no known competing financial interests or personal relationships that could have appeared to influence the work reported in this paper.

CRediT authorship contribution statement

Congcong Bian: Investigation, Writing - original draft. **Huimin Wang:** Writing - original draft. **Xueli Zhang:** Visualization. **Sa Xiao:** Supervision. **Zhuang Liu:** Formal analysis. **Xia Wang:** Conceptualization, Resources, Writing - review & editing.

Acknowledgments

This work was supported by grants from National Key Research and Development Program of China (2019YFA0904800), National Natural Science Foundation of China (91951202 and 31570103), and Shandong Science & Technology Fund Planning Project (2019GSF109069).

Appendix A. Supplementary data

Supplementary data to this article can be found online at https://doi.org/10.1016/j.bios.2019.111985.

References

Alfonso, D.R., 2008. Surf. Sci. 602, 2758–2768.
Allen, M.J., Tung, V.C., Kaner, R.B., 2010. Chem. Rev. 110, 132–145.
Becerril, H.A., Mao, J., Liu, Z.F., Stoltenberg, R.M., Bao, Z.N., Chen, Y.S., 2008. ACS Nano 2, 463–470.
Brito, J.A., Sousa, F.L., Stelter, M., Bandeiras, T.M., Vonrhein, C., Teixeira, M., Pereira, M.M., Archer, M., 2009. Biochemistry 48, 5613–5622.
Canbay, E., Habip, A., Kara, G., Eren, Z., Akyilmaz, E., 2015. Food Chem. 169, 197–202.
Chang, J.B., Zhou, G.H., Christensen, E.R., Heideman, R., Chen, J.H., 2014. Anal. Bioanal. Chem. 406, 3957–3975.
Cherney, M.M., Zhang, Y.F., Solomonson, M., Weiner, J.H., James, M.N.G., 2010. J. Mol. Biol. 398, 292–305.
Cui, L., Wu, J., Ju, H.X., 2015. Biosens. Bioelectron. 63, 276–286.
Dai, L.M., 2013. Accounts Chem. Res. 46, 31–42.
Dong, X., Li, M., Feng, N., Sun, Y., Yang, C., Xu, Z., 2015. RSC Adv. 5, 86485–86489.
Feng, H., Huang, Z., Lou, X., Li, J., Hui, G., 2017. Food Anal. Method. 10, 407–418.
Gao, X.Y., Gao, Y., Bian, C.C., Ma, H.Y., Liu, H.L., 2019. Electrochim. Acta 310, 78–85.
García-Calzada, M., Marbán, G., Fuertes, A.B., 1999. Anal. Chim. Acta 380, 39–45.
Ge, X.B., Wang, L.Q., Liu, Z.N., Ding, Y., 2011. Electroanalysis 23, 381–386.
Hui, G., Lu, H., Jiang, Z., Zhu, D., Wan, H., 2017. Biosens. Bioelectron. 97, 184–195.
Jin, W., Wu, G.S., Chen, A.C., 2014. Analyst 139, 235–241.
Kumar, J., D'Souza, S.F., 2011. Biosens. Bioelectron. 26, 4289–4293.
Liu, J., Chen, J.H., Fang, Z.Y., Zeng, L.W., 2012. Analyst 137, 5502–5505.
Liu, Q., Wang, H., Li, H., Zhang, J., Zhuang, S., Zhang, F., Hsia, K.J., Wang, P., 2013. Biosens. Bioelectron. 40, 174–179.
Liu, Z., Ma, H.Y., Sun, H.H., Gao, R., Liu, H.L., Wang, X., Xu, P., Xun, L.Y., 2017. Biosens. Bioelectron. 98, 29–35.
Lu, Y., Li, H., Zhuang, S., Zhang, D., Zhang, Q., Zhou, J., Dong, S., Liu, Q., Ping Wang, P., 2014. Sens. Actuators B 193, 420–427.
Lu, Y., Yao, Y., Zhang, Q., Zhang, D., Zhuang, S., Li, H., Liu, Q., 2015. Biosens. Bioelectron. 67, 662–669.
Ma, Y.L., Zhao, J.L., Yang, B.L., 2006. Int. Biodeterior. Biodegrad. 57, 93–98.
Manavalan, S., Rajaji, U., Chen, S.M., Govindasamy, M., Selvin, S.S.P., Chen, T.W., Ali, M.A., Al-Hemaid, F.M.A., Elshikh, M.S., 2019. Ultrason. Sonochem. 51, 103–110.
Milby, T.H., Baselt, R.C., 1999. Am. J. Ind. Med. 35, 192–195.
Peng, B., Chen, W., Liu, C.R., Rosser, E.W., Pacheco, A., Zhao, Y., Aguilar, H.C., Xian, M., 2014. Chem. Eur J. 20, 1010–1016.
Poor, N.Z.M., Baniasadi, L., Omidi, M., Amoabediny, G., Yazdian, F., Attar, H., Heydarzadeh, A., Zarami, A.S.H., Sheikhha, M.H., 2014. Enzym. Microb. Technol. 63, 7–12.
Qiu, C.C., Wang, X., Liu, X.Y., Hou, S.F., Ma, H.Y., 2012. Electrochim. Acta 67, 140–146.
Van Staden, J.F., Kluever, L.G., 1998. Anal. Chim. Acta 369, 157–161.
Vycudilik, W., 1985. Forensic Sci. Int. 28, 131–136.

Wang, X., Liu, X.Y., Yan, X.L., Zhao, P., Ding, Y., Xu, P., 2011. PLoS One 6, e24207.
Wu, C., Liu, Z., Sun, H.H., Wang, X., Xu, P., 2016. Biosens. Bioelectron. 79, 843–849.
Xin, Y.F., Liu, H.L., Cui, F.F., Liu, H.W., Xun, L.Y., 2016. Environ. Microbiol. 18, 5123–5136.
Xu, T.L., Scafa, N., Xu, L.P., Zhou, S.F., Al-Ghanem, K.A., Mahboob, S., Fugetsu, B., Zhang, X.J., 2016. Analyst 141, 1185–1195.
Yan, X.L., Meng, F.H., Cui, S.Z., Liu, J.G., Gu, J., Zou, Z.G., 2011. J. Electroanal. Chem. 661, 44–48.
Yu, Y.Y., Liu, X.M., Wang, H.Y., Li, X.T., Lin, J.Q., 2014. J. Bacteriol. 196, 2255–2264.
Zhang, D., Lu, Y., Zhang, Q., Yao, Y., Li, S., Li, H., Zhuang, S., Jiang, J., Gang Logan Liu, G.L., Liu, Q., 2015. Sens. Actuators B 221, 341–349.
Zhang, X., Zhao, Z., Lou, X., Li, J., Hui, G., 2017. J. Food Meas. Charact. 11, 548–555.
Zhang, Y.F., Qadri, A., Weiner, J.H., 2016. Biochem. Cell Biol. 94, 159–166.